Simulations of Emission Spectra for LH4 Ring - Fluctuations in Radial Positions of Molecules

Pavel Heřman, David Zapletal

***Abstract*—**Results of computer simulation of steady state fluorescence spectra and absorption ones for ring molecular systems are presented. The peripheral cyclic antenna unit LH4 of the bacterial photosystem from purple bacteria can be modeled by such system. The cumulant-expansion method of Mukamel et al. is used for the calculation of spectral responses of the system with exciton-phonon coupling. Dynamic disorder, interaction with a bath, in Markovian approximation simultaneously with uncorrelated static disorder in radial positions of molecules are taking into account in our simulations. Also localization of exciton states is studied and discussed. We compare calculated results for LH4 ring obtained within the full Hamiltonian model with our previous results within the nearest neighbour approximation model. Comparison with the results calculated within different types of uncorrelated static disorder is also done.

***Keywords*—**LH4, absorption and fluorescence spectrum, static and dynamic disorder, exciton states, localization

I. Introduction

IN the process of photosynthesis (in plants, bacteria, and blue-green algae), solar energy is used to split water and produce oxygen molecules, protons and electrons. Photosynthesis starts with the absorption of a solar photon which is absorbed by a complex system of membrane-associated pigment-proteins (light-harvesting (LH) antenna) and absorbed energy is efficiently transferred to a reaction center (RC), where it is converted into a chemical energy [1]. These initial ultrafast events have been extensively investigated. Knowledge of the microscopic structure of some photosynthetic systems, e.g., photosynthetic systems of purple bacteria, invokes during last twenty years long and intensive effort of many theoretical and experimental laboratories. Our interest is mainly focused on first (light) stage of photosynthesis in purple bacteria.

Manuscript received December 19, 2014.

This work was supported in part by the Faculty of Science, University of Hradec Králové (project of specific research No. 2106/2014 - P. Heřman).

P. Heřman is with the Department of Physics, Faculty of Science, University of Hradec Králové, Rokitanského 62, 50003 Hradec Králové, Czech Republic (e-mail: pavel.herman@uhk.cz).

D. Zapletal is with the Institute of Mathematics and Quantitative Methods, Faculty of Economics and Administration, University of Pardubice, Studentská 95, 53210 Pardubice, Czech Republic (e-mail: david.zapletal@upce.cz).

The antenna systems of photosynthetic units from purple bacteria are formed by ring units LH1, LH2, LH3, and LH4. Their geometric structures are known in great detail from X-ray crystallography. The general organization of above mentioned light-harvesting complexes is the same: identical subunits are repeated cyclically in such a way that a ring-shaped structure is formed. However the symmetries of these rings are different.

The core antenna LH1 contained in purple bacteria such as *Rhodopseudomonas palustris* consists of approximately 16 structural subunits in which two bacteriochlorophyll *a* (BChl-*a*) molecules are noncovalently attached to pairs of transmembrane polypeptides. These subunits are arranged in a ringlike structure which surround the RC. In the near infrared LH1 absorbs at 870 nm. More about crystal structure of this core complex is possible to find e.g. in [2].

Crystal structure of LH2 complex contained in purple bacterium Rhodopseudomonas acidophila in high resolution was first described by McDermott et al. [3] in 1995, then further e.g. by Papiz et al. [4] in 2003. Bacteriochlorophyll (BChl) molecules are organized in two concentric rings. One ring features a group of nine well-separated BChl molecules (B800) with absorption band at about 800 nm. The other ring consists of eighteen closely packed BChl molecules (B850) absorbing around 850 nm. LH2 complexes from other purple bacteria have analogous ring structure.

Some bacteria express also other types of complexes such as the B800-820 LH3 complex (*Rhodopseudomonas acidophila* strain 7050) or the LH4 complex (*Rhodopseudomonas palustris*). LH3 complex like LH2 one is usually nonameric but LH4 one is octameric. While the B850 dipole moments in LH2 ring have tangential arrangement, in the LH4 ring they are oriented more radially. Mutual interactions of the nearest neighbour BChls in LH4 are approximately two times smaller in comparison with LH2 and have opposite sign. The other difference is the presence of an additional BChl ring in LH4 complex [5]. Different arrangements manifest themselves in different optical properties. At this article we mainly focus on LH4 complex.

The intermolecular distances under 1 nm determine strong exciton couplings between corresponding pigments. Due to the strong interaction between BChl molecules, an extended Frenkel exciton states model is considered in our theoretical approach. Despite intensive

study of bacterial antenna systems, e.g. [3]–[6], the precise role of the protein moiety for governing the dynamics of the excited states is still under debate. At room temperature the solvent and protein environment fluctuates with characteristic time scales ranging from femtoseconds to nanoseconds. The simplest approach is to substitute fast fluctuations by dynamic disorder and slow fluctuation by static disorder.

In our previous papers we presented results of simulations doing within the nearest neighbour approximation model. In several steps we extended the former investigations of static disorder effect on the anisotropy of fluorescence made by Kumble and Hochstrasser [7] and Nagarajan et al. [8]–[10] for LH2 ring. After studying the influence of diagonal dynamic disorder for simple systems (dimer, trimer) [11]–[13], we added this effect into our model of LH2 ring by using a quantum master equation in Markovian and non-Markovian limits [14]–[16]. We also studied influence of four types of uncorrelated static disorder [17], [18] (Gaussian disorder in local excitation energies, Gaussian disorder in transfer integrals, Gaussian disorder in radial positions of BChls and Gaussian disorder in angular positions of BChls on the ring). Influence of correlated static disorder, namely an elliptical deformation of the ring, was also taken into account [14]. We also investigated the time dependence of fluorescence anisotropy for the LH4 ring with different types of uncorrelated static disorder [16], [19].

Recently we have focused on the modeling of absorption and steady state fluorescence spectra. Our results for LH2 and LH4 rings within the nearest neighbour approximation model have been presented in [20]–[25]. The results for LH2 and LH4 ring within full Hamiltonian model have been published in [26]–[32].

Present paper is the extension of our contribution presented on WSEAS and NAUN conference ASM'14 [33]. Main goal of the paper is the comparison of the results for LH4 ring calculated within full Hamiltonian model with our previous results calculated within the nearest neighbour approximation model. The rest of the paper is organized as follows. Section II introduces the ring model with the static disorder and dynamic disorder (interaction with phonon bath). Also the cumulant expansion method, which is used for the calculation of spectral responses of the system with exciton-phonon coupling, is described there. Computational point of view is mentioned in Section III. The results of our simulations and used units and parameters could be found in Section IV. Some conclusions are drawn in Section V.

II. Physical model

We assume that only one exciton is present on the ring after an impulsive excitation. The Hamiltonian of the exciton in the ideal ring coupled to a bath of harmonic oscillators reads

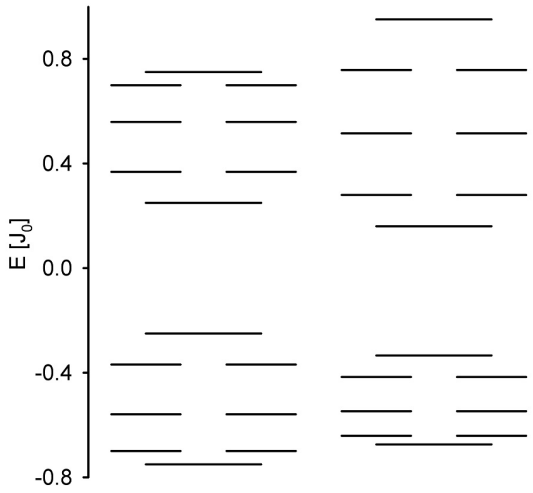

Fig. 1. Energetic band structure of the ring from LH4 (left column - the nearest neighbour approximation model, right column - full Hamiltonian model.

$$H^0 = H^0_{\rm ex} + H_{\rm ph} + H_{\rm ex-ph}. \tag{1}$$

Here the first term,

$$H^0_{\rm ex} = \sum_{m,n(m\neq n)} J_{mn} a^\dagger_m a_n, \tag{2}$$

corresponds to an exciton, e.g. the system without any disorder. The operator $a^\dagger_m$ (a_m) creates (annihilates) an exciton at site m, J_{mn} (for $m \neq n$) is the so-called transfer integral between sites m and n. The second term,

$$H_{\rm ph} = \sum_q \hbar\omega_q b^\dagger_q b_q, \tag{3}$$

represents phonon bath in harmonic approximation (the phonon creation and annihilation operators are denoted by $b^\dagger_q$ and b_q, respectively). Last term in (1),

$$H_{\rm ex-ph} = \frac{1}{\sqrt{N}} \sum_m \sum_q G^m_q \hbar\omega_q a^\dagger_m a_m (b^\dagger_q + b_q), \tag{4}$$

describes exciton-phonon interaction which is assumed to be site-diagonal and linear in the bath coordinates (the term G^m_q denotes the exciton-phonon coupling constant).

Inside one ring the pure exciton Hamiltonian can be diagonalized using the wave vector representation with corresponding delocalized "Bloch" states α and energies E_α. Assuming the nearest neighbour approximation model (only the nearest neighbour transfer matrix elements are considered) and homogeneous case, transfer integrals read

$$J_{mn} = J_0(\delta_{m,n+1} + \delta_{m,n-1}). \tag{5}$$

Using Fourier transformed excitonic operators (Bloch representation)

$$a_\alpha = \sum_n a_n \mathrm{e}^{\mathrm{i}\alpha n}, \tag{6}$$

where

$$\alpha = \frac{2\pi}{N} l,\ l = 0, \pm 1, \ldots, \pm\frac{N}{2}, \tag{7}$$

the form of the simplest exciton Hamiltonian in α - representation is

$$H^0_{\mathrm{ex}} = \sum_\alpha E_\alpha a^\dagger_\alpha a_\alpha, \tag{8}$$

with

$$E_\alpha = -2J_0 \cos\alpha. \tag{9}$$

LH4 ring is not perfectly homogeneous but it is significantly dimerized. Energetic band structure of such dimerized ring in case of the nearest neighbour approximation model can be seen in Figure 1 - left column. For full Hamiltonian model (full transfer matrix is taken into account in dipole-dipole approximation) energetic band structure slightly differs (Figure 1 - right column). Differences of energies in lower part of the band are smaller and in upper part of the band are larger in comparison with the nearest neighbour approximation model.

Influence of uncorrelated static disorder is modeled by fluctuations δr_n in radial positions of bacteriochlorophyll molecules on the ring with Gaussian distribution and standard deviation Δ_r The Hamiltonian H_{s} of the uncorrelated static disorder adds to the Hamiltonian H^0_{ex}.

The cumulant-expansion method of Mukamel et al. [34], [35] is used for the calculation of spectral responses of the system with exciton-phonon coupling. Absorption $OD(\omega)$ and steady-state fluorescence $FL(\omega)$ spectrum can be expressed as

$$OD(\omega) = \omega \sum_\alpha d^2_\alpha \times \times \mathrm{Re}\int_0^\infty dt \mathrm{e}^{\mathrm{i}(\omega-\omega_\alpha)t - g_{\alpha\alpha\alpha\alpha}(t) - R_{\alpha\alpha\alpha\alpha}t}, \tag{10}$$

$$FL(\omega) = \omega \sum_\alpha P_\alpha d^2_\alpha \times \times \mathrm{Re}\int_0^\infty dt \mathrm{e}^{\mathrm{i}(\omega-\omega_\alpha)t + \mathrm{i}\lambda_{\alpha\alpha\alpha\alpha}t - g^*_{\alpha\alpha\alpha\alpha}(t) - R_{\alpha\alpha\alpha\alpha}t}. \tag{11}$$

Here

$$\vec{d_\alpha} = \sum_n c^\alpha_n \vec{d_n} \tag{12}$$

is the transition dipole moment of eigenstate α, c^α_n are the expansion coefficients of the eigenstate α in site representation and P_α is the steady state population of the eigenstate α. The inverse lifetime of exciton state $R_{\alpha\alpha\alpha\alpha}$ is given by the elements of Redfield tensor $R_{\alpha\beta\gamma\delta}$ [36]. It is a sum of the relaxation rates between exciton states,

$$R_{\alpha\alpha\alpha\alpha} = -\sum_{\beta\neq\alpha} R_{\beta\beta\alpha\alpha}. \tag{13}$$

The g-function and λ-values in (11) are given by

$$g_{\alpha\beta\gamma\delta} = -\int_{-\infty}^{\infty} \frac{d\omega}{2\pi\omega^2} C_{\alpha\beta\gamma\delta}(\omega) \times \times \left[\coth\frac{\omega}{2k_{\mathrm{B}}T}(\cos\omega t - 1) - \mathrm{i}(\sin\omega t - \omega t)\right], \tag{14}$$

$$\lambda_{\alpha\beta\gamma\delta} = -\lim_{t\to\infty}\frac{d}{dt}\mathrm{Im}\{g_{\alpha\beta\gamma\delta}(t)\} = = \int_{-\infty}^{\infty}\frac{d\omega}{2\pi\omega} C_{\alpha\beta\gamma\delta}(\omega). \tag{15}$$

The matrix of the spectral densities $C_{\alpha\beta\gamma\delta}(\omega)$ in the eigenstate (exciton) representation reflects one-exciton states coupling to the manifold of nuclear modes. In what follows only a diagonal exciton phonon interaction in site representation is used (see (1)), i.e., only fluctuations of the pigment site energies are assumed and the restriction to the completely uncorrelated dynamical disorder is applied.

In such case each site (i.e. each chromophore) has its own bath completely uncoupled from the baths of the other sites. Furthermore it is assumed that these baths have identical properties [15], [37], [38]

$$C_{mnm'n'}(\omega) = \delta_{mn}\delta_{mm'}\delta_{nn'}C(\omega). \tag{16}$$

After transformation to the exciton representation we have

$$C_{\alpha\beta\gamma\delta}(\omega) = \sum_n c^\alpha_n c^\beta_n c^\gamma_n c^\delta_n C(\omega). \tag{17}$$

Various models of spectral density of the bath are used in literature [39]–[41]. In our present investigation we have used the model of Kühn and May [40]

$$C(\omega) = \Theta(\omega) j_0 \frac{\omega^2}{2\omega_c^3}\mathrm{e}^{-\omega/\omega_c} \tag{18}$$

which has its maximum at $2\omega_c$.

Localization of the exciton states contributing to the steady state fluorescence spectrum can be characterized by the thermally averaged participation ratio $\langle PR\rangle$, which is given by

$$\langle PR\rangle = \frac{\sum_\alpha PR_\alpha\ \mathrm{e}^{-\frac{E_\alpha}{k_B T}}}{\sum_\alpha \mathrm{e}^{-\frac{E_\alpha}{k_B T}}}, \tag{19}$$

where

$$PR_\alpha = \sum_{n=1}^{N} |c^\alpha_n|^4. \tag{20}$$

III. Computational point of view

To obtain absorption and steady state fluorescence spectra it is necessary to calculate single ring $OD(\omega)$ and $FL(\omega)$ spectra for large number of different static disorder realizations created by random number generator. Finally these results have to be averaged over all realizations of static disorder.

For our previous calculations of absorption and fluorescence spectra (for uncorrelated static disorder in local excitation energies $\delta\varepsilon_n$ and transfer integrals δJ_{mn}) software package *Mathematica* [42]–[44] was used. But standard numerical integration method used in *Mathematica* proved to be unsuitable in case of full Hamiltonian model and static disorder in radial positions of molecules δr_n. It was not possible to achieve satisfactory convergence by above mentioned integration method from *Mathematica*. This is the reason a procedure in Fortran was created for present calculations. Integrated functions are oscillating and damped (see (10) and (11)). That is why the functions were integrated as sums of contributions from individual cycles of oscillation. Predetermined accuracy could be achieved by integration over finite time interval $t \in \langle 0, t_0\rangle$ (instead of $\langle 0, \infty)$). If

$$t_0 \geq \max\{t_\alpha\}, \quad \alpha = 1, \ldots, 18, \tag{21}$$

where t_α satisfy condition (Q is arbitrary real positive number)

$$t_\alpha \geq \frac{1}{R_{\alpha\alpha\alpha\alpha}} \ln\left(\frac{18\omega d_\alpha^2}{QR_{\alpha\alpha\alpha\alpha}}\right), \tag{22}$$

then deviations of $OD(\omega)$ and $FL(\omega)$ from precise values are not larger then Q. $OD(\omega)$ and $FL(\omega)$ are

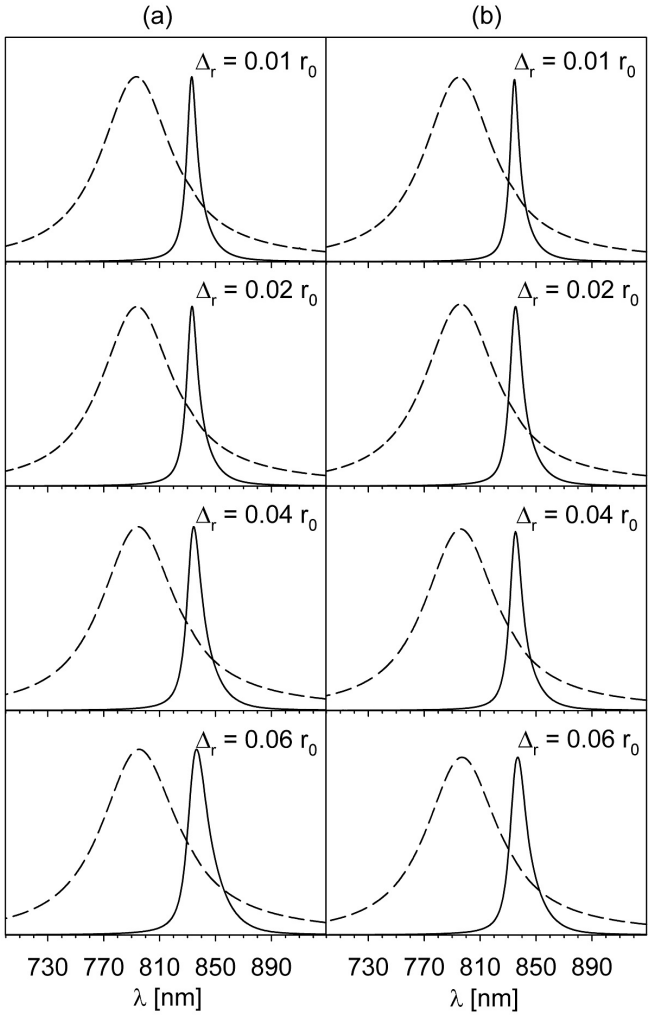

Fig. 2. Calculated $FL(\omega)$ and $OD(\omega)$ spectra at low temperature $kT = 0.1\ J_0$ averaged over 2000 realizations of static disorder in radial positions of molecules δr_n (four strengths $\Delta_r = 0.01,\ 0.02,\ 0.04, 0.06\ r_0$), full Hamiltonian model - (a), the nearest neighbour approximation model - (b).

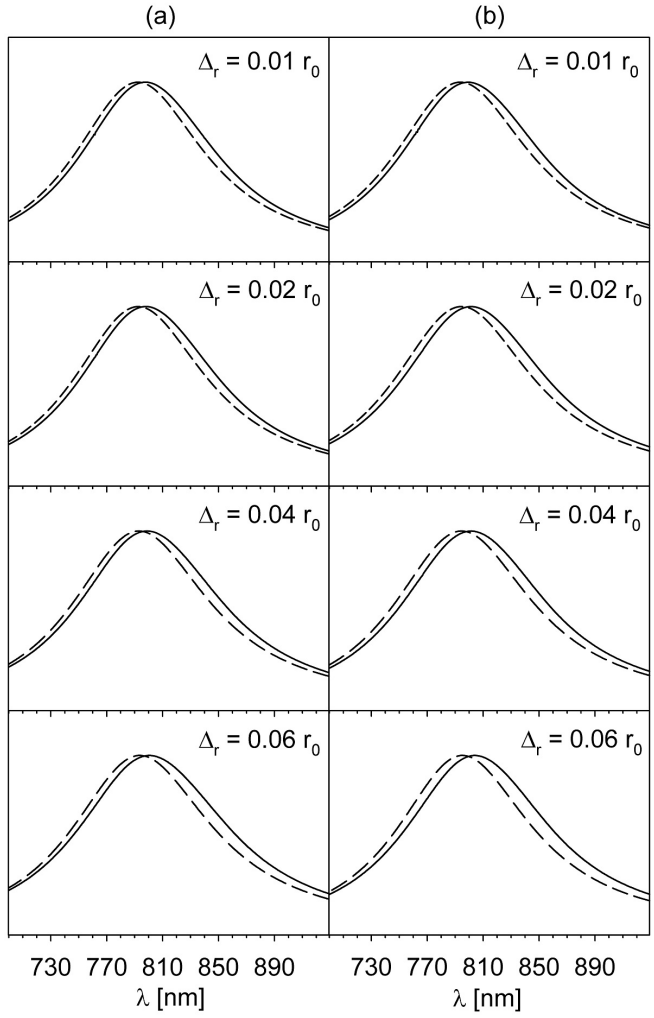

Fig. 3. Calculated $FL(\omega)$ and $OD(\omega)$ spectra at room temperature $kT = 0.5\ J_0$ averaged over 2000 realizations of static disorder in radial positions of molecules δr_n (four strengths $\Delta_r = 0.01,\ 0.02,\ 0.04, 0.06\ r_0$), full Hamiltonian model - (a), the nearest neighbour approximation model - (b).

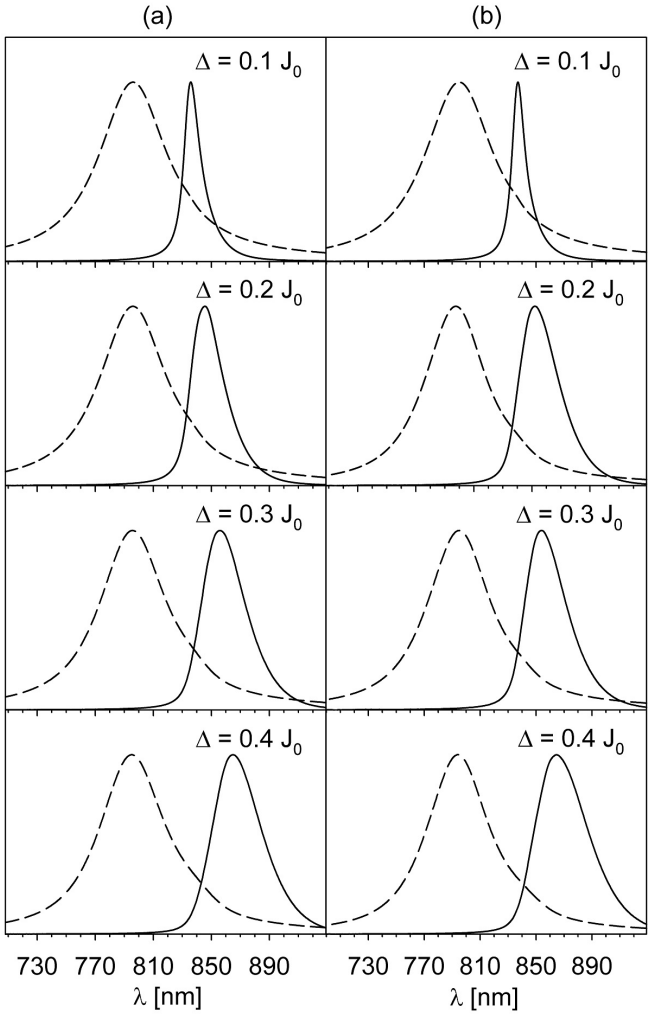

Fig. 4. Calculated $FL(\omega)$ and $OD(\omega)$ spectra at low temperature $kT = 0.1\ J_0$ averaged over 2000 realizations of static disorder in local excitation energies $\delta\varepsilon_n$ (four strengths $\Delta = 0.1,\ 0.2,\ 0.3, 0.4\ J_0$), full Hamiltonian model - (a), the nearest neighbour approximation model - (b).

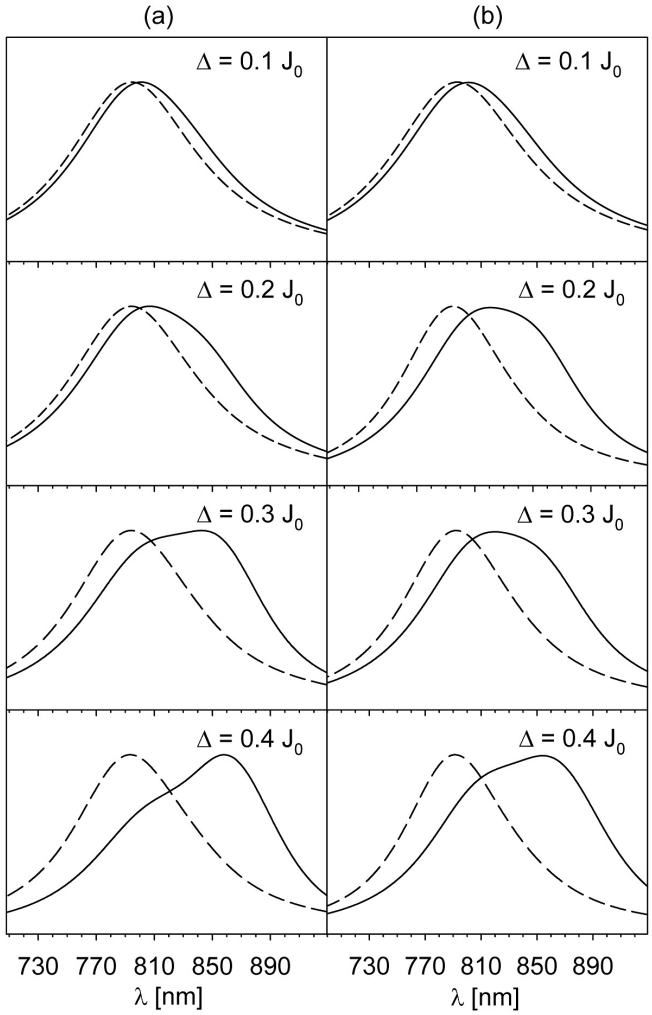

Fig. 5. Calculated $FL(\omega)$ and $OD(\omega)$ spectra at room temperature $kT = 0.5\ J_0$ averaged over 2000 realizations of static disorder in local excitation energies $\delta\varepsilon_n$ (four strengths $\Delta = 0.1,\ 0.2,\ 0.3, 0.4\ J_0$), full Hamiltonian model - (a), the nearest neighbour approximation model - (b).

therefore integrated as sums of contributions from individual cycles of oscillation until upper limit of integration exceeds t_0.

IV. Results

Above mentioned type of uncorrelated static disorder, e.g. fluctuations of radial positions of molecules on the ring, has been taken into account in our simulations simultaneously with dynamic disorder in Markovian approximation. Resulting absorption and steady state fluorescence spectra for LH4 ring obtained within the full Hamiltonian model are compared with our previous results calculated within the nearest neighbour approximation model.

Dimensionless energies normalized to J_0 (the transfer integral between the nearest neighbour bacteriochlorophylls in LH2 ring) have been used. Estimation of J_0 varies in literature between $250\ \mathrm{cm}^{-1}$ and $400\ \mathrm{cm}^{-1}$. The nearest neighbour transfer integrals in LH4 ring have opposite sign in comparison with those of LH2 ring and differ also in their absolute values. Furthermore, stronger dimerization can be found in LH4 ring in comparison with LH2 ring [5]. Therefore we have taken the values of the nearest neighbour transfer integrals in LH4 ring as follows: $J_{12}^{LH4} = -0.5 J_{12}^{LH2} = -0.5 J_0$, $J_{23}^{LH4} = 0.5 J_{12}^{LH4} = -0.25 J_0$. All our simulations of LH4 spectra have been done with the same values of $J_0 = 400\ \mathrm{cm}^{-1}$ and unperturbed transition energy from the ground state $E_0 = 12300\ \mathrm{cm}^{-1}$, that we found for LH2 ring (the nearest neighbour approximation model) [21]. The model of spectral density of Kühn and May [12] has been used in our simulations. In agreement with our previous results [17], [45] we have used the strength of dynamic disorder $j_0 = 0.4\ J_0$ and cut–off frequency

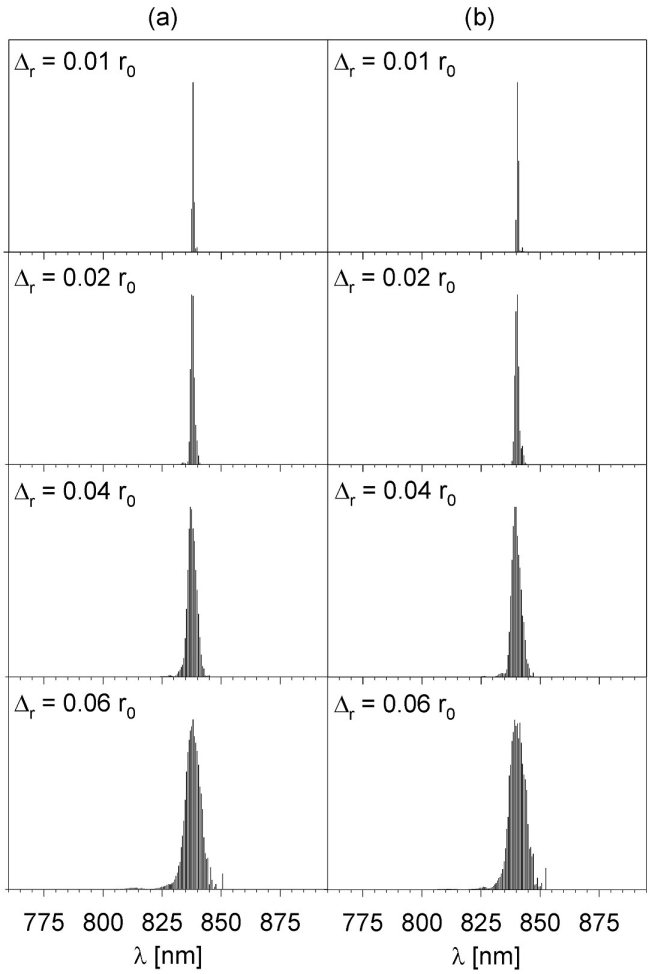

Fig. 6. The distributions of the quantity $P_\alpha d_\alpha^2$ at low temperature $kT = 0.1\ J_0$ as a function of wavelength λ for 2000 realizations of static disorder in radial positions of molecules δr_n (four strengths $\Delta_r = 0.01,\ 0.02,\ 0.04, 0.06\ r_0$), full Hamiltonian model - (a), the nearest neighbour approximation model - (b).

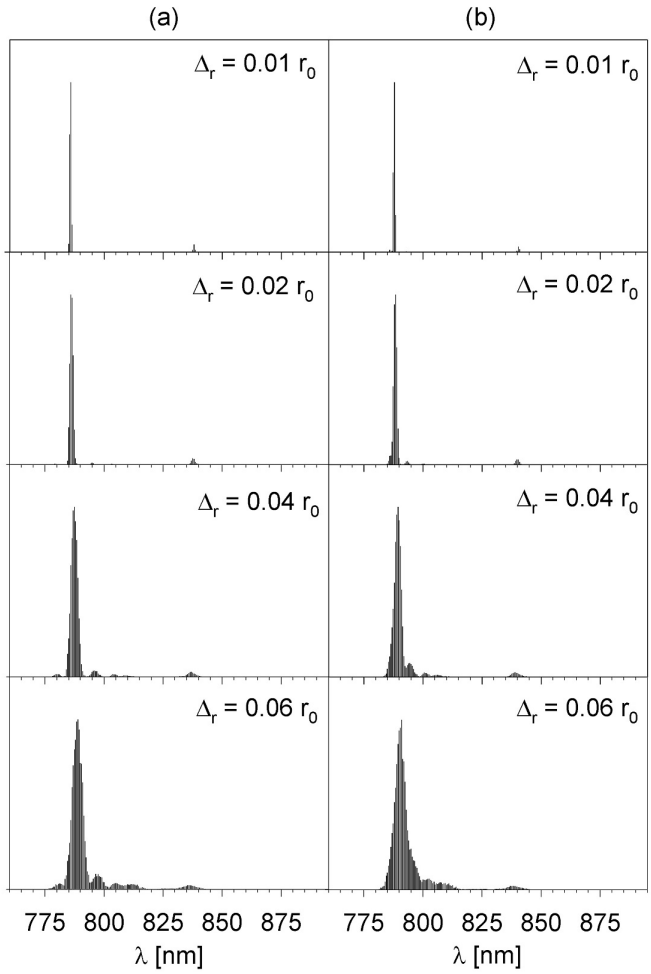

Fig. 7. The distributions of the quantity $P_\alpha d_\alpha^2$ at room temperature $kT = 0.5\ J_0$ as a function of wavelength λ for 2000 realizations of static disorder in radial positions of molecules δr_n (four strengths $\Delta_r = 0.01,\ 0.02,\ 0.04, 0.06\ r_0$), full Hamiltonian model - (a), the nearest neighbour approximation model - (b).

$\omega_c = 0.212\ J_0$ (see (18)).

Resulting absorption $OD(\omega)$ and steady state fluorescence spectra $FL(\omega)$ averaged over 2000 realizations of static disorder in radial positions of molecules δr_n for both models (full Hamiltonian model and the nearest neighbour approximation one) can be seen in Figure 2 (low temperature $kT = 0.1\ J_0$) and in Figure 3 (room temperature $kT = 0.5\ J_0$). The strengths of uncorrelated static disorder in radial positions of molecules Δ_r have been taken in agreement with [46], i.e. $\Delta_r \in \langle 0.01\ r_0,\ 0.06\ r_0 \rangle$. Four strengths $\Delta_r = 0.01,\ 0.02,\ 0.04,\ 0.06\ r_0$ have been chosen in our calculations.

For comparison, absorption spectra $OD(\omega)$ and steady state fluorescence spectra $FL(\omega)$ averaged over 2000 realizations of static disorder in local excitation energies $\delta\varepsilon_n$ ($\Delta = 0.1,\ 0.2,\ 0.3,\ 0.4\ J_0$) for both models (full Hamiltonian model and the nearest neighbour approximation one) [28] are presented in Figure 4 (low temperature $kT = 0.1\ J_0$) and in Figure 5 (room temperature $kT = 0.5\ J_0$).

In addition, the distributions of the quantity $P_\alpha d_\alpha^2$ (P_α is the steady state population of the eigenstate α, d_α^2 is the dipole strength of eigenstate α, see (11)) as a function of wavelength λ have been investigated. The distributions of this quantity for 2000 realizations of uncorrelated static disorder in radial positions of molecules δr_n for both models (full Hamiltonian model and the nearest neighbour approximation one) are presented in Figure 6 (low temperature $kT = 0.1\ J_0$) and in Figure 7 (room temperature $kT = 0.5\ J_0$). The same, but for 2000 realizations of uncorrelated static disorder in local excitation energies $\delta\varepsilon_n$ are shown in Figure 8 (low temperature $kT = 0.1\ J_0$) and in Figure 9 (room temperature $kT = 0.5\ J_0$).

Localization of exciton states in LH4 ring was studied

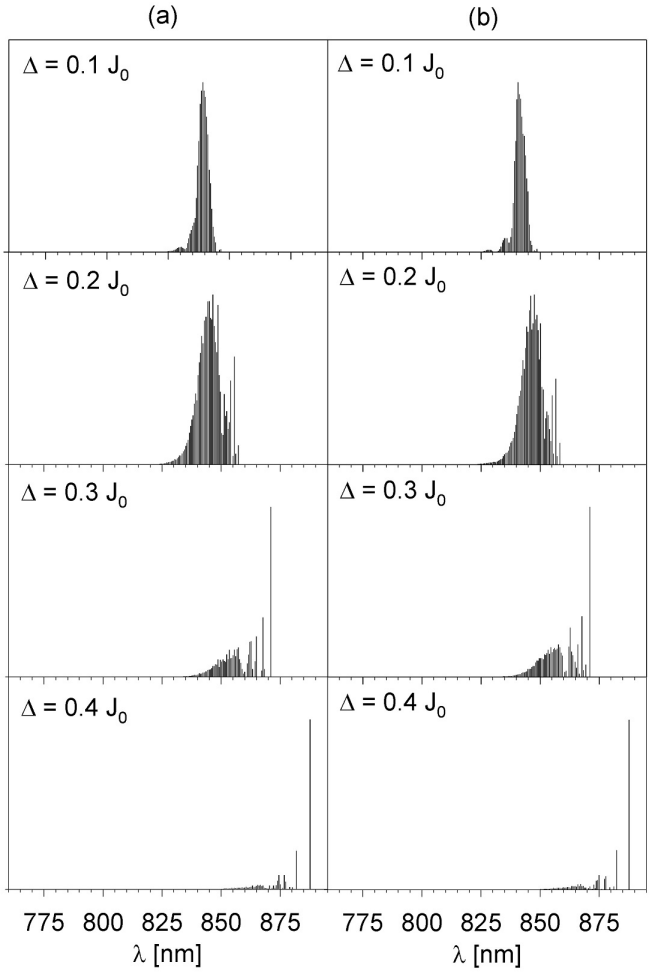

Fig. 8. The distributions of the quantity $P_\alpha d_\alpha^2$ at low temperature $kT = 0.1\ J_0$ as a function of wavelength λ for 2000 realizations of static disorder in local excitation energies $\delta\varepsilon_n$ (four strengths $\Delta = 0.1,\ 0.2,\ 0.3, 0.4\ J_0$), full Hamiltonian model - (a), the nearest neighbour approximation model - (b).

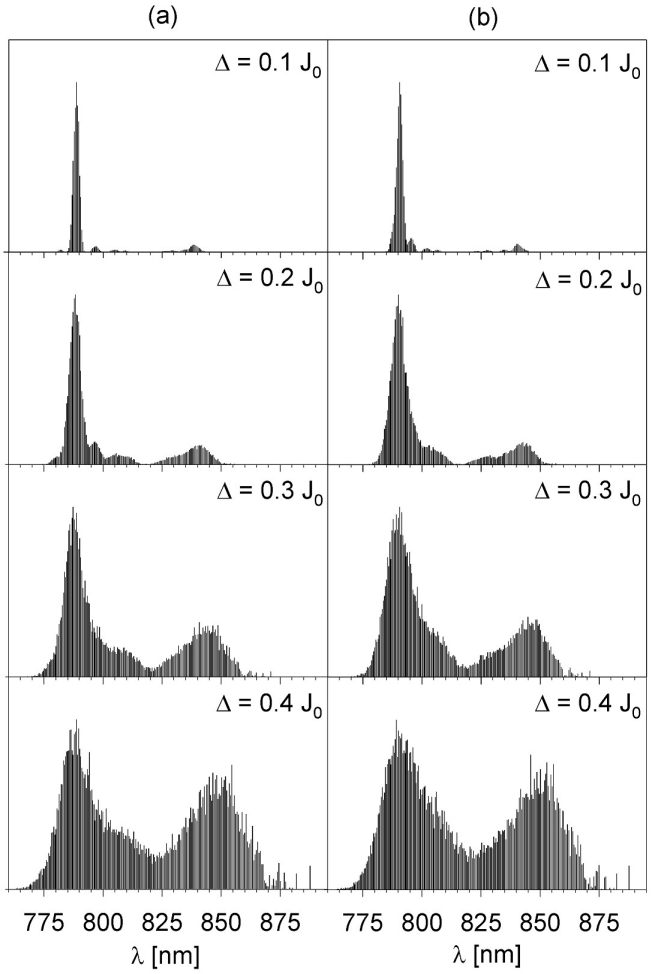

Fig. 9. The distributions of the quantity $P_\alpha d_\alpha^2$ at room temperature $kT = 0.5\ J_0$ as a function of wavelength λ for 2000 realizations of static disorder in local excitation energies $\delta\varepsilon_n$ (four strengths $\Delta = 0.1,\ 0.2,\ 0.3, 0.4\ J_0$), full Hamiltonian model - (a), the nearest neighbour approximation model - (b).

by means of the thermally averaged participation ratio $\langle PR\rangle$. The distributions of $\langle PR\rangle$ values as functions of single ring fluorescence spectrum peak position calculated for 2000 realizations of static disorder δr_n in radial positions of molecules on the ring are shown in Figure 10 (low temperature $kT = 0.1\ J_0$) and Figure 11 (room temperature $kT = 0.5\ J_0$).

V. Conclusions

From the comparison of our simulated $FL(\omega)$ and $OD(\omega)$ spectra for LH4 ring within full Hamiltonian model with our previous results calculated within the nearest neighbour approximation one we can make following conclusions.

Any substantial differences between the results for full Hamiltonian model and the nearest neighbour approximation one (Figure 2 and Figure 3) are not visible for static disorder in radial positions of molecules. Only in case of low temperature ($kT = 0.1\ J_0$) fluorescence spectral lines are slightly wider for full Hamiltonian model (Figure 2 (a)) in comparison with the nearest neighbour approximation one (Figure 2 (b)).

On the other hand, comparison of the results for uncorrelated static disorder in radial positions of molecules with the results for other types of static disorder gives essential difference at room temperature ($kT = 0.5\ J_0$). Contrary to the case of static disorder in radial positions the splitting of fluorescence spectral line appears for static disorder in local excitation energies [23] (see Figure 5) and static disorder in transfer integrals [25] (mainly for the nearest neighbour approximation model). This conclusion is supported also by the distributions of the quantity $P_\alpha d_\alpha^2$ (Figure 6 - Figure 9). In case of static disorder in radial positions (Figure 6 and Figure 7) only one strong peak is visible in distributions of this

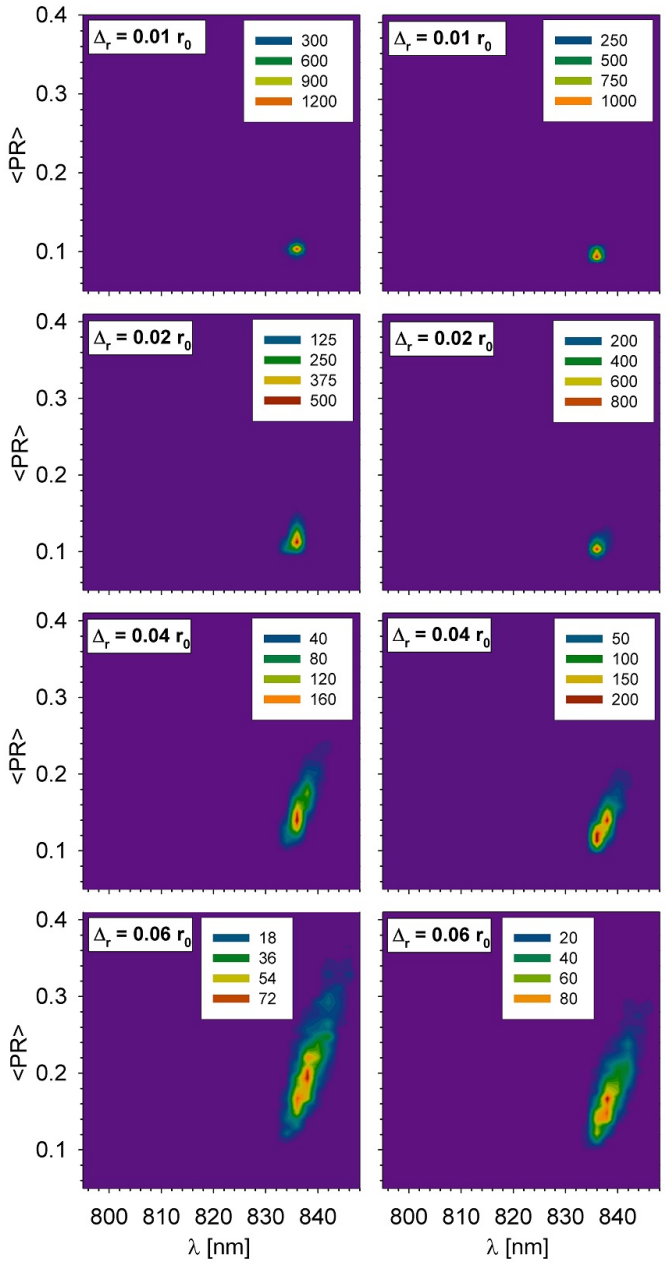

Fig. 10. The distributions of $\langle PR \rangle$ values as a function of single ring steady state $FL(\omega)$ spectrum peak position at low temperature $kT = 0.1\ J_0$ calculated for 2000 realizations of Gaussian uncorrelated static disorder in radial positions of molecules δr_n (four strengths $\Delta_r = 0.01,\ 0.02,\ 0.04,\ 0.06\ r_0$), full Hamiltonian model – left column, the nearest neighbour approximation model – right column.

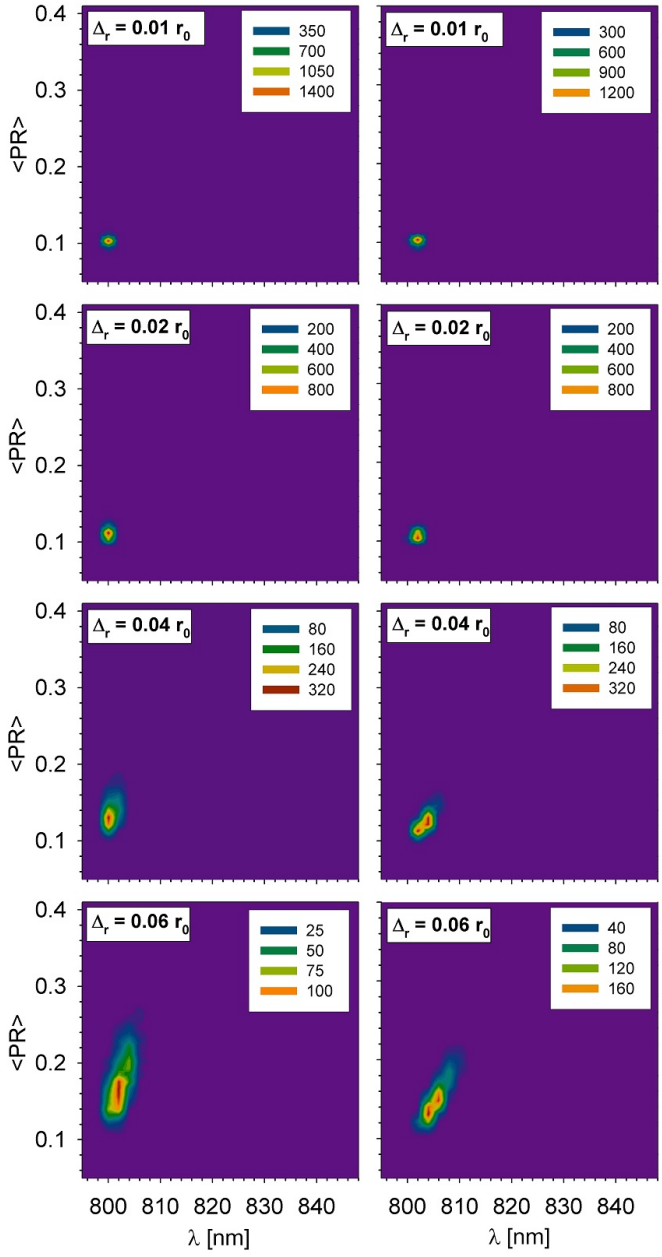

Fig. 11. The distributions of $\langle PR \rangle$ values as a function of single ring steady state $FL(\omega)$ spectrum peak position at room temperature $kT = 0.5\ J_0$ calculated for 2000 realizations of Gaussian uncorrelated static disorder in radial positions of molecules δr_n (four strengths $\Delta_r = 0.01,\ 0.02,\ 0.04,\ 0.06\ r_0$), full Hamiltonian model – left column, the nearest neighbour approximation model – right column.

quantity. In contrast with this type of static disorder, the second strong peak appears in case of static disorder in local excitation energies for room temperature (Figure 9). Without any static disorder only two upper exciton degenerate states closest to the state with the highest energy (see Figure 1) are optically active, i.e. have nonzero dipole strengths. The dipole strengths of the states with lower energies (higher wavelengths) become nonzero with growing static disorder strength. That is why the second peak in the distribution of the quantity $P_\alpha d_\alpha^2$ becomes more significant with growing strength of static disorder.

The fluorescence spectral line splitting appears also for LH2 ring but for low temperature ($kT = 0.1\ J_0$) and full Hamiltonian model. Unlike the LH4 ring the fluorescence spectral line splitting in case of LH2 ring

is visible not only for static disorder in local excitation energies [26] and in transfer integrals [30], but also for the static disorder in radial positions of molecules [31].

For LH4 ring substantial differences between considered models of Hamiltonian in case of static disorder in radial positions are not clear either from the distributions of $\langle PR \rangle$ values (Figure 10 and Figure 11). Thermally averaged participation ratio $\langle PR \rangle$ depends on temperature (see (19)). For room temperature, higher exciton states have higher probabilities of occupation in comparison with low temperature. That is why the distributions are shifted to higher energies (lower wavelengths) in case of room temperature. In addition, the range of $\langle PR \rangle$ values is wider and reaches higher values for low temperature, i.e. localization of exciton states is slightly higher in this case (for both models of Hamiltonian).

REFERENCES

[1] R. van Grondelle, V. I. Novoderezhkin, "Energy transfer in photosynthesis: experimental insights and quantitative models", *Physical Chemistry Chemical Physics* 8, 2003, pp. 793–807.

[2] A.W. Roszak et al., "Crystal structure of the RC-LH1 core complex from Rhodopseudomonas palustris", *Science* 302, 2003, pp. 1976–1972.

[3] G. McDermott, S.M. Prince, A.A. Freer, A.M. Hawthornthwaite-Lawless, M.Z. Papiz, R.J. Cogdell, N.W. Isaacs, "Crystal structure of an integral membrane light-harvesting complex from photosynthetic bacteria", *Nature* 374, 1995, pp. 517–521.

[4] M.Z. Papiz, S.M. Prince, T. Howard, R.J. Cogdell, N.W. Isaacs, "The structure and thermal motion of the B 800850 LH2 complex from Rps. acidophila at 2.0 A resolution and 100 K: new structural features and functionally relevant motions", *J. Mol. Biol.* 326, 2003, pp. 1523–1538

[5] W.P.F. de Ruijter, et al., "Observation of the Energy-Level Structure of the Low-Light Adapted B800 LH4 Complex by Single-Molecule Spectroscopy", *Biophys. J.* 87, 2004, pp. 3413–3420.

[6] R. Kumble, R. Hochstrasser, "Disorder-induced exciton scattering in the light-harvesting systems of purple bacteria: Influence on the anisotropy of emission and band $\rightarrow$ band transitions", *J. Chem. Phys.* 109, 1998, pp. 855–865.

[7] V. Nagarajan et al., "Ultrafast exciton relaxation in the B850 antenna complex of Rhodobacter sphaeroides", *Proc. Natl. Acad. Sci. USA* 93, 1996, pp. 13774–13779.

[8] V. Nagarajan et al., "Femtosecond pump-probe spectroscopy of the B850 antenna complex of Rhodobacter sphaeroides at room temperature", *J. Phys. Chem. B* 103, 1999, pp. 2297–2309.

[9] V. Nagarajan, W. W. Parson, "Femtosecond fluorescence depletion anisotropy: Application to the B850 antenna complex of Rhodobacter sphaeroides", *J. Phys. Chem. B* 104, 2000, pp. 4010–4013.

[10] V. Čápek, I. Barvík, P. Heřman, "Towards proper parametrization in the exciton transfer and relaxation problem: dimer", *Chem. Phys.* 270, 2001, pp. 141–156.

[11] P. Heřman, I. Barvík, "Towards proper parametrization in the exciton transfer and relaxation problem. II. Trimer", *Chem. Phys.* 274, 2001, pp. 199–217.

[12] P. Heřman, I. Barvík, M. Urbanec, "Energy relaxation and transfer in excitonic trimer", *J. Lumin.* 108, 2004, pp. 85–89.

[13] P. Heřman et al., "Exciton scattering in light-harvesting systems of purple bacteria", *J. Lumin.* 94-95, 2001, pp. 447–450.

[14] P. Heřman, I. Barvík, "Non-Markovian effects in the anisotropy of emission in the ring antenna subunits of purple bacteria photosynthetic systems", *Czech. J. Phys.* 53, 2003, pp. 579–605.

[15] P. Heřman et al., "Influence of static and dynamic disorder on the anisotropy of emission in the ring antenna subunits of purple bacteria photosynthetic systems", *Chem. Phys.* 275, 2002, pp. 1–13.

[16] P. Heřman, I. Barvík, "Temperature dependence of the anisotropy of fluorescence in ring molecular systems", *J. Lumin.* 122–123, 2007, pp. 558–561.

[17] P. Heřman, I. Barvík, "Coherence effects in ring molecular systems", *Phys. Stat. Sol. C* 3, 2006, 3408–3413.

[18] P. Heřman, D. Zapletal, I. Barvík, "The anisotropy of fluorescence in ring units III: Tangential versus radial dipole arrangement", *J. Lumin.* 128, 2008, pp. 768–770.

[19] P. Heřman, I. Barvík, D. Zapletal, "Computer simulation of the anisotropy of fluorescence in ring molecular systems: Tangential vs. radial dipole arrangement", *Lecture Notes in Computer Science* 5101, 2008, pp. 661–670.

[20] P. Heřman, D. Zapletal, J. Šlégr, "Comparison of emission spectra of single LH2 complex for different types of disorder", *Phys. Proc.* 13, 2011, pp. 14–17.

[21] P. Heřman, D. Zapletal, M. Horák, "Computer simulation of steady state emission and absorption spectra for molecular ring", in *Proc. 5th International Conference on Advanced Engineering Computing and Applications in Sciences (ADVCOMP2011)*, Lisbon: IARIA, 2011, pp. 1–6.

[22] D. Zapletal, P. Heřman, "Simulation of molecular ring emission spectra: localization of exciton states and dynamics", *Int. J. Math. Comp. Sim.* 6, 2012, pp. 144–152.

[23] M. Horák, P. Heřman, D. Zapletal, "Simulation of molecular ring emission spectra - LH4 complex: localization of exciton states and dynamics", *Int. J. Math. Comp. Sim.* 7, 2013, pp. 85–93.

[24] M. Horák, P. Heřman, D. Zapletal, "Modeling of emission spectra for molecular rings - LH2, LH4 complexes", *Phys. Proc.* 44, 2013, pp. 10–18.

[25] P. Heřman, D. Zapletal, "Intermolecular coupling fluctuation effect on absorption and emission spectra for LH4 ring", *Int. J. Math. Comp. Sim.* 7, 2013, pp. 249–257.

[26] P. Heřman, D. Zapletal, M. Horák, "Emission spectra of LH2 complex: full Hamiltonian model", *Eur. Phys. J. B* 86, 2013, art. no. 215.

[27] D. Zapletal, P. Heřman, "Photosynthetic Complex LH2 - Absorption and Steady State Fluorescence Spectra", in *Proc. of 6th Int. Conf. on Sust. Energy and Env. Protect. (SEEP2013)*, Maribor, 2013, pp. 284–290.

[28] P. Heřman, D. Zapletal, "Emission Spectra of LH4 Complex: Full Hamiltonian Model", *Int. J. Math. Comp. Sim.* 7, 2013, pp. 448-455.

[29] P. Heřman, D. Zapletal, "Simulation of Emission Spectra for LH4 Ring: Intermolecular Coupling Fluctuation Effect", *Int. J. Math. Comp. Sim.* 8, 2014, pp. 73-81.

[30] D. Zapletal, P. Heřman, "Photosynthetic complex LH2 - Absorption and steady state fluorescence spectra", *Energy* 77, 2014, pp. 212-219.

[31] P. Heřman, D. Zapletal, P. Kabrhel, "Photosynthetic Complex LH4 - Absorption and Steady State Fluorescence Spectra", in *Recent Advances in Mathematical Methods in Applied Sciences, Proc. of the 2014 Int. Conf. on Mathematical Models and Methods in Applied Sciences (MMAS '14)*, Saint Petersburg, 2014, pp. 96-101.

[32] D. Zapletal, P. Heřman, "Photosynthetic Complex LH4 - Absorption and Steady State Fluorescence Spectra", in *Proc. of 7th Int. Conf. on Sust. Energy and Env. Protect. (SEEP2014)*, Dubai, 2014, Art. no. 67.

[33] P. Heřman, D. Zapletal, J. Šlégr, "Simulations of Absorption and Emission Spectra for LH4 Ring - Full Hamiltonian Model", in *Recent Advances in Applied Mathematics, Modelling and Simulation, Proc. of the 8th Int. Conf. on Applied Mathematics, Simulation, Modelling (ASM '14)*, Florence, 2014, pp. 286-294.

[34] W. M. Zhang et al., "Exciton-migration and three-pulse femtosecond optical spectroscopies of photosynthetic antenna complexes", *J. Chem. Phys.* 108, 1998, pp. 7763–7774.

[35] S. Mukamel, *Principles of nonlinear optical spectroscopy*. New York: Oxford University Press, 1995.

[36] A. G. Redfield, "The Theory of Relaxation Processes", *Adv. Magn. Reson.* 1, 1965, pp. 1–32.

[37] D. Rutkauskas et al., "Fluorescence spectroscopy of conformational changes of single LH2 complexes", *Biophys. J.* 88, 2005, pp. 422–435.

[38] D. Rutkauskas et al., "Fluorescence spectral fluctuations of single LH2 complexes from *Rhodopseudomonas acidophila* strain 10050", *Biochemistry* 43, 2004, pp. 4431–4438.

[39] V. I. Novoderezhkin, D. Rutkauskas, R. van Grondelle, "Dynamics of the emission spectrum of a single LH2 complex: Interplay of slow and fast nuclear motions", *Biophys. J.* 90, 2006, pp. 2890–2902.

[40] V. May, O. Kühn, *Charge and Energy Transfer in Molecular Systems*. Berlin: Wiley-WCH, 2000.

[41] O. Zerlauskiene et al., "Static and Dynamic Protein Impact on Electronic Properties of Light-Harvesting Complex LH2", *J. Phys. Chem. B* 112, 2008, pp. 15883–15892.

[42] S. Wolfram, *The Mathematica Book*, 5th ed., Wolfram Media, 2003.

[43] M. Trott, *The Mathematica GuideBook for Symbolics*. New York: Springer Science+Business Media, Inc., 2006.

[44] M. Trott, *The Mathematica GuideBook for Numerics*. New York: Springer Science+Business Media, Inc., 2006.
[45] P. Heřman, D. Zapletal, I. Barvík, "Lost of coherence due to disorder in molecular rings", *Phys. Stat. Sol. C* 6, 2009, 89–92.
[46] P. Heřman, I. Barvík, D. Zapletal, "Energetic disorder and exciton states of individual molecular rings", *J. Lumin.* 119-120, 2006, pp. 496–503.